bioRxiv preprint doi: https://doi.org/10.1101/804559; this version posted October 14, 2019. The copyright holder for this preprint (which was not certified by peer review) is the author/funder. All rights reserved. No reuse allowed without permission.

Allosteric communications between domains modulate activity of matrix metalloprotease-1

Lokender Kumar[1], Anthony Nash[2], Chase Harms[1], Joan Planas[3], Derek Wright[1], Judith Klein-Seetharaman[3,4], and Susanta K. Sarkar[1,*]

[1]*Department of Physics, Colorado School of Mines, USA*
[2]*Nuffield Department of Clinical Neurosciences, University of Oxford, UK*
[3]*Warwick Medical School, University of Warwick, UK*
[4]*Department of Chemistry, Colorado School of Mines, USA*

Corresponding author:
[*]ssarkar@mines.edu

ABSTRACT

The relation between structure and dynamics of biomolecules is important for their functions. Intra-domain dynamics occurring at pico- to milli-second timescales have been shown to correlate with activity. However, the correlation of allosteric communications between domains with biomolecular function is poorly understood. Here we show that inter-domain dynamics of matrix metalloprotease-1 (MMP1) on collagen fibrils are correlated with activity. Using single-molecule FRET, we identified the functionally relevant conformations where the two MMP1 domains are far apart, which were significantly absent for inactive MMP1 and could be modulated by inhibitor and enhancer of activity. All-atom and coarse-grained simulations reproduced the experimental features and revealed that dynamics are similar at pico- and milli-second timescales and substrate-dependent. Functional conformations are accompanied by larger catalytic pocket openings, which are increased by the communications mediated by collagen even if the domain linker is absent. Inter-domain communications are likely important for multidomain proteins in general.

Keywords: Inter-domain dynamics and activity, MMP1 conformational dynamics on type-1 collagen fibrils, Allosteric communications mediated by substrate, Single-molecule FRET.

bioRxiv preprint doi: https://doi.org/10.1101/804559; this version posted October 14, 2019. The copyright holder for this preprint (which was not certified by peer review) is the author/funder. All rights reserved. No reuse allowed without permission.

The roles of protein conformational dynamics in activity are debated with arguments both in favor[1] and against[2]. A direct link between the hierarchies of conformational dynamics timescales from pico- to milli-second has been argued based on experimental and computational studies[3]. However, the debate has not been fully resolved. Collagen degradation by MMP1 provides a unique opportunity to define the relation of conformational dynamics with activity of a protein because both the catalytic and hemopexin domains of MMP1 are necessary to degrade structurally intact collagen[4]. Collagen is the primary component of the extracellular matrix (ECM) that provides a scaffold for cells to maintain tissue integrity. Degradation of fibrils by matrix metalloproteases (MMPs) is an integral part of tissue remodeling. MMP1, a collagenase in the 23-member MMP family, can degrade the most abundant type-1 collagen. MMP1 consists of a catalytic domain that degrades collagen, a hemopexin domain that helps MMPs bind to collagen, and a linker that mediates communications between the two domains. Interestingly, the catalytic domain sequence of MMP1 is very similar to other MMPs in the family, suggesting that differences in activity and substrate specificity among MMPs are likely caused by allosteric (far from the catalytic site) communications from other domains. Most studies have been reported with soluble collagen monomers. Each 300 nm long collagen monomer with a 1.5 nm diameter consists of three left-handed chains forming a right-handed triple-helical structure that hides the cleavage sites and makes collagen resistant to degradation. Biochemical studies with monomer revealed that MMP1 actively unwinds the three chains of a monomer[5]. Using MD studies, the same results were reinterpreted and argued that collagen itself "breathes", i.e. it partially unwinds itself due to thermal fluctuations, enabling MMP1 to bind and cleave collagen[6], a conclusion for which additional experimental support was reported[7]. Indeed, computational and experimental studies revealed conformational dynamics between the catalytic and hemopexin domains of MMP1[8]. It should be noted that although the MMP1 catalytic domain alone (where the hemopexin domain has been truncated) can degrade denatured collagen (the cleavage sites are easily accessible), it cannot degrade the basic building block of collagen fibrils, i.e., triple-helical collagen (the cleavage sites are not easily accessible)[4]. Thus, both the hemopexin and catalytic domains are needed for degradation suggesting possible roles of inter-domain motions in activity. However, studies with collagen monomers do not reveal the complete information about physiologically important collagen fibrils for several reasons. First, collagen fibrils are insoluble and macroscopic, greatly complicating ensemble biochemical and kinetics studies. Fibrils are larger than MMPs in size and MMPs bind fibrils nonspecifically as well as at the partially unwound vulnerable sites on fibrils created during fibril assembly[9,10]. As such, binding to the cleavage sites is not a simple diffusion-limited process determined by the diffusion constant in solution. Also, the combined MMP1-fibril system is not statistically time-independent because the fibril itself changes as it is degraded by MMP1. Second, as monomers self-assemble into fibrils, the cleavage sites become less accessible compared to monomers due to covering by the C-terminal telopeptides[11]. Saffarian et al.[12] showed that collagen degradation biases the motion of MMP1 on type-1 collagen fibrils using Fluorescence Correlation Spectroscopy (FCS). Using single-molecule tracking of labeled MMP1 on type-1 collagen fibrils, we showed that MMP1 diffusion is both biased and hindered due to cleavage[10]. MMP1 spends more than 90% of its time on the collagen fibril by diffusing, binding, and pausing without initiating degradation. Such extensive binding and pausing effectively regulate the rate of degradation and reduces the apparent catalytic rate of MMP1. The subsequent publication showed that fibrils also play a role in MMP1 activity due to vulnerable sites on fibrils caused by relaxation of strain during fibril assembly[9]. These results lead to the hypothesis that the overall catalytic rate of MMP1 depends not only on active site catalysis, but also on diffusive motion[10], substrate

bioRxiv preprint doi: https://doi.org/10.1101/804559; this version posted October 14, 2019. The copyright holder for this preprint (which was not certified by peer review) is the author/funder. All rights reserved. No reuse allowed without permission.

properties[9], and conformational dynamics. Here we show that functionally relevant MMP1 conformations have the catalytic and hemopexin domains far apart. These conformations are present in active MMP1 but significantly absent in inactive MMP1. These conformations are inhibited by tetracycline, an antibiotic that is known to inhibit MMP1 activity as well. In contrast, low FRET conformations are enhanced by MMP9, which can degrade denatured collagen but cannot degrade triple-helical collagen. Molecular dynamics simulations of active and inactive MMP1 bound to a model triple-helical collagen reproduce the experimental observations. Experimentally-validated MD simulations further revealed that MMP1 opens up its catalytic domain more compared to inactive MMP1. In addition, the root mean square (rms) distance between the MMP1 catalytic site and the cleavage sites on the collagen chains has a lower average value for active MMP1 compared to inactive MMP1.

Results and discussion

Single-molecule measurement of MMP1 inter-domain dynamics on reconstituted type-1 collagen fibril. For our studies, we differentiated the role of activity by comparing the results for active (E219) with catalytically inactive (E219Q) MMP1. We mutated SER142 on the catalytic domain and SER366 on the hemopexin domain to cysteines (**Figure 1A**). Note that the amino acid E219[13] is the same as E200[5], which differs due to the first residue used for counting. The distance between the central carbon atoms of the two selected amino acids is ~4.5 nm, which is similar to the Förster radius of the dye pair Alexa Fluor® 555 and Alexa Fluor® 647. We labeled MMP1 with Alexa555 and Alexa647 using maleimide chemistry. The left panel of **Figure 1B** shows the gel electrophoresis of labeled MMP1, whereas the right panel (**Figure 1B**) shows the specific activities of labeled and unlabeled MMP1 on the synthetic peptide substrate, MCA-Lys-Pro-Leu-Gly-Leu-DPA-Ala-Arg-NH_2[14]. Labeling did not affect the activity of MMP1. We used a Total Internal Reflection Fluorescence (TIRF) microscope because many MMPs can be imaged simultaneously, in contrast to a confocal microscope with point-detection. We used the TIRF microscope in prism-type configuration (**Figure 1C**) because it has low background due to the separation of excitation and emission paths, in contrast to the objective-type TIRF microscope where the excitation and emission path share optics. As labeled MMPs moved and underwent inter-domain dynamics on the surface of a fibril, fluorescence emissions from the donor and acceptor dyes were detected using two quadrants (channels) of the EMCCD camera. Two channels were superimposed and the intensity and location of spots were tracked to measure both the diffusive motion and measure inter-domain dynamics) of MMP1. If there was relative motion between the MMP1 domains, energy transferred from Alexa555 to Alexa647 due to FRET, increasing the emission from Alexa647 and simultaneously reducing the emission from Alexa555. An example of anticorrelated emission from the two dyes due to MMP1 inter-domain dynamics is shown in **Figure 1D**. See Methods for detailed procedures.

bioRxiv preprint doi: https://doi.org/10.1101/804559; this version posted October 14, 2019. The copyright holder for this preprint (which was not certified by peer review) is the author/funder. All rights reserved. No reuse allowed without permission.

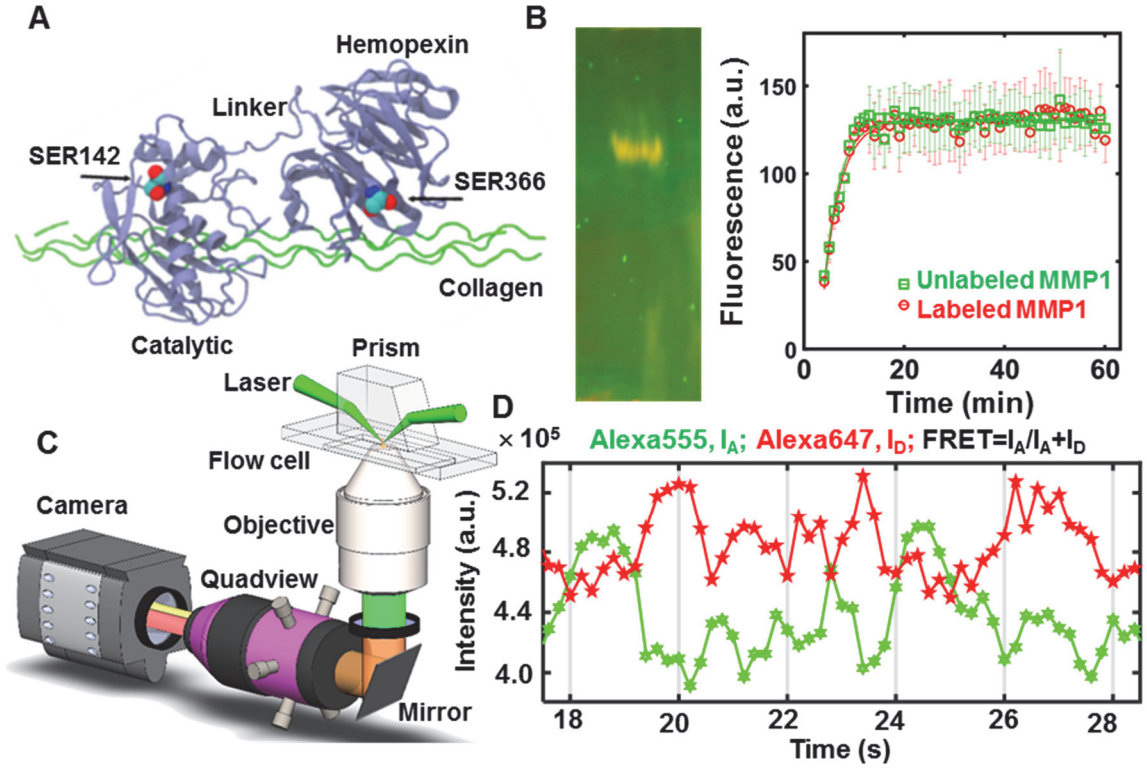

Figure 1. Single-molecule measurement of MMP1 dynamics on type-1 collagen fibril. (**A**) Relative positions of the domains and serine residues mutated to cysteines for labeling (created using PDB ID 4AUO). (**B**) Left panel: 12% SDS PAGE of labeled MMP1; Right panel: Fluorescence from degraded peptide substrate as a function of time for unlabeled (green squares) and labeled (red circles) MMP1 at 37ºC. Solid lines are respective best fits to $y=a-b*\exp(-kt)$. After calibration, the specific activity is ~1000 pmol/min/μg. The error bars are the standard deviations of 3 technical repeats. (**C**) Schematics of the TIRF microscope. (**D**) Emission intensities of the two dyes. Low FRET conformations lead to high Alexa555 emission, whereas High FRET conformations lead to Low Alexa555 emission. Anticorrelated Alexa647 and Alexa555 emissions, I_A and I_D respectively, indicate conformational dynamics of MMP1.

Inter-domain dynamics and activity of MMP1 are functionally related. The role of dynamics in activity is not clear: Warshel proposes that protein dynamics and enzyme catalysis are not coupled[2,15], but Karplus proposes that enzyme motions can lower the activation energy[1,3]. Single-molecule measurements of inter-domain dynamics (**Figure 2**) of active and inactive MMP1 suggest that the low FRET conformations, where two domains are far apart, are relevant for catalysis. To further delineate the relation between conformations and activity, we used two ligands: MMP9 and tetracycline. MMP9, another member of the MMP family that can degrade denatured collagen, is generally thought to be unable to degrade triple-helical type-1 collagen[16]. MMP9 can be found in both pro-form[17,18] and activated forms[19-22] in physiological conditions. It has been reported that MMP9 and MMP1 form a stable complex[23] and computational studies have predicted enhancement of MMP1 activity[24]. Tetracycline has been shown to play dual roles as antibiotics and MMP inhibitors[25].

bioRxiv preprint doi: https://doi.org/10.1101/804559; this version posted October 14, 2019. The copyright holder for this preprint (which was not certified by peer review) is the author/funder. All rights reserved. No reuse allowed without permission.

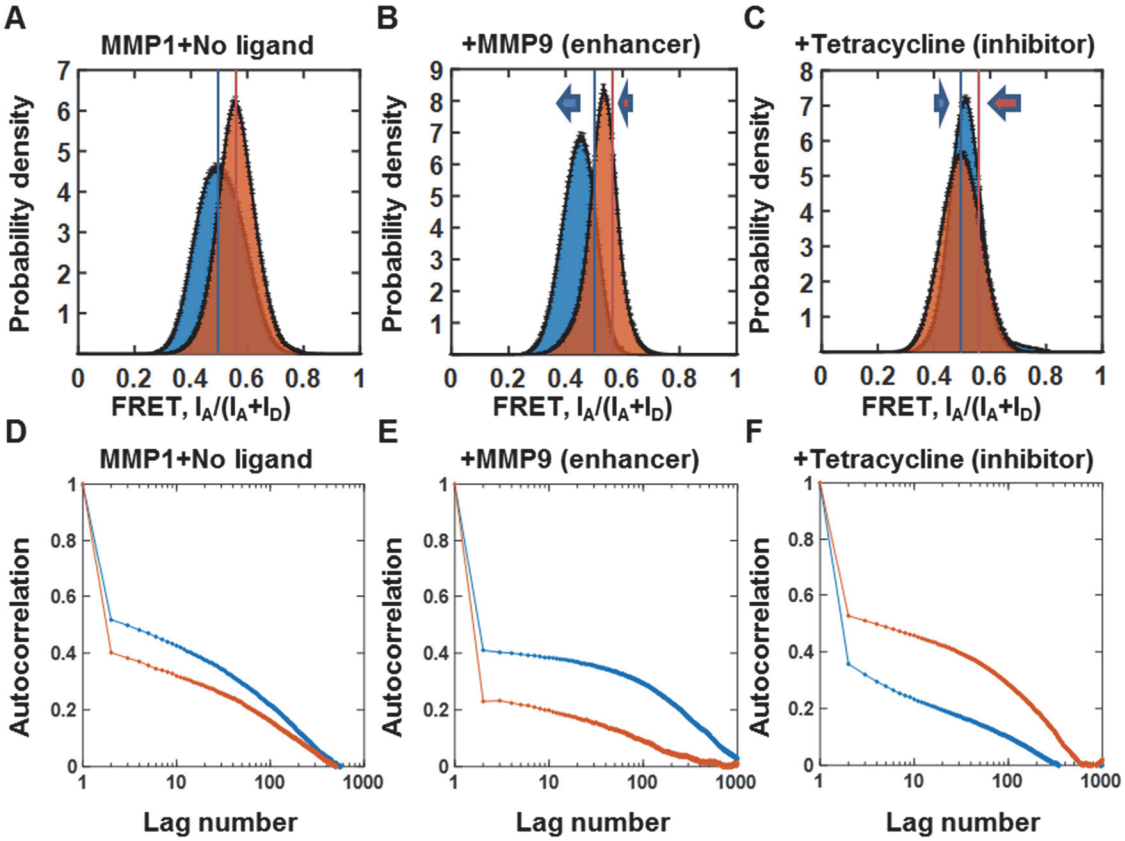

Figure 2. Activity-dependent inter-domain dynamics of MMP1 on reconstituted type-1 collagen fibrils at 22ºC with 100 ms time resolution. Area-normalized histograms of MMP1 inter-domain distance (more than 300,000 FRET values for each condition; bin size=0.005) for active (blue) and inactive (orange) MMP1 (**A**) without ligand, (**B**) in the presence of MMP9 (an enhancer), and (**C**) in the presence of tetracycline (an inhibitor). The error bars in histograms represent the square roots of histogram bin counts. Blue and orange lines indicate the peak positions for active and inactive MMP1 without ligands. Low FRET conformations, where the inter-domain distance is larger, are functionally important. Autocorrelation of MMP1 inter-domain distance for active (blue) and inactive (orange) MMP1 (**D**) without ligand, (**E**) in the presence of MMP9, and (**E**) in the presence of tetracycline. The error bars in autocorrelations represent the standard error of mean calculated from individual FRET trajectories.

In the presence of MMP9, which forms a complex with MMP1 and has been predicted to enhance MMP1 activity[24], the peaks of conformational histograms shift towards left (indicated by arrows) as shown in **Figure 2B**. MMP9 not only enables more low FRET conformations of MMP1, but it also stabilizes low FRET conformations as indicated by narrow widths of histograms (**Figure 2B**) and longer correlation times (**Figure 2E**). In contrast, tetracycline inhibits low FRET conformations and appears to shift conformations for both active and inactive MMP1 towards the middle (**Figure 2C**). Since correlated motions indicate a decrease conformational entropy and can affect kinetics and thermodynamics of biological processes including catalysis[26], we calculated autocorrelation function of MMP1 conformational dynamics under different experimental conditions (**Figures 2D-2F**). Without any ligand, active MMP1 had more time-correlated conformational dynamics than inactive MMP1 (**Figure 2D**). In the presence of MMP9, the time-correlations were longer for both active and inactive MMP1 (**Figure 2E**). Interestingly,

bioRxiv preprint doi: https://doi.org/10.1101/804559; this version posted October 14, 2019. The copyright holder for this preprint (which was not certified by peer review) is the author/funder. All rights reserved. No reuse allowed without permission.

tetracycline reversed the trend and inactive MMP1 had longer time-correlation than active MMP1 (**Figure 2F**). Taken together, these results strongly suggest that inter-domain dynamics and activity of MMP1 are functionally related. Nevertheless, a larger inter-domain distance could be a "consequence" or the "cause" of catalytic activity. We argue that low FRET conformations are likely the "cause" for several reasons. First, a mutation E219Q at the catalytic site not only renders MMP1 inactive, but it also induces changes far away (allosteric) to alter the inter-domain dynamics. Second, changes in the linker region also have been shown to affect activity allosterically[27]. Third, the catalytic domains of MMPs are largely conserved[28], suggesting a key role of the hemopexin domains in human MMPs can lead to substrate specificity[29] via allosteric inter-domain communications. Fourth, although the MMP1 catalytic domain alone (where the hemopexin domain has been truncated) can degrade denatured collagen (the cleavage sites are easily accessible), it cannot degrade the basic building block of collagen fibrils, i.e., triple-helical collagen (the cleavage sites are not easily accessible)[4,30,31]. Thus, both the hemopexin and catalytic domains are needed for triple-helical collagen degradation.

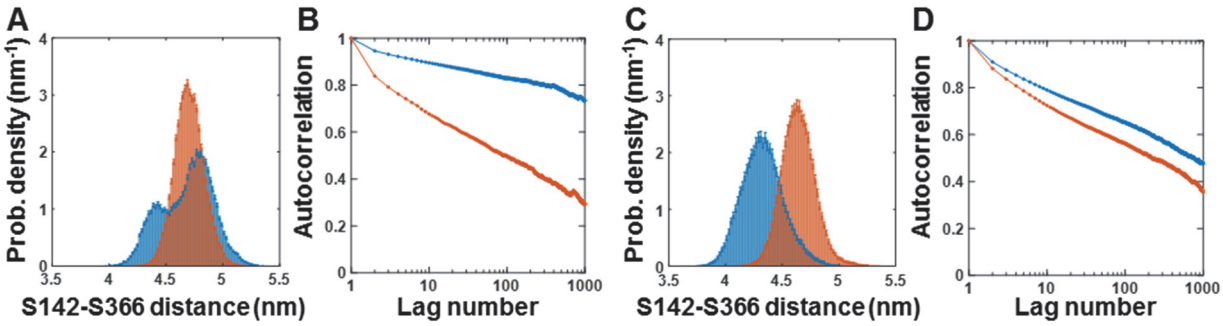

Figure 3. All-atom MD simulations with collagen backbone restrained (A and B) and unrestrained (C and D). Modified GROMACS topology files used in the previously published work by Nash et al. [64] were used for simulations at 37ºC with 2 fs time step; data saved every 5 ps; 225 ns and 700 ns simulations for restrained and unrestrained respectively. Area-normalized simulated histograms with bin size=0.02 (**A**) and autocorrelation function (**B**) for active (blue) and inactive (orange) when the collagen backbone was restrained with an energy penalty of 1000 kJ/mol. Area-normalized simulated histograms (**C**) and autocorrelation function (**D**) for active (blue) and inactive (orange) when the collagen backbone was unrestrained.

MMP1 conformations are similar at two extreme timescales and change upon substrate binding. The MMP1 catalytic cleft (~0.5 nm wide) is too narrow to accommodate the collagen monomer (1.5 nm in diameter)[8]. Therefore, a larger opening of the MMP1 catalytic pocket is needed to accommodate collagen and must accompany a larger inter-domain dynamics if low FRET conformations are indeed important. To this end, we confirmed the activity-dependent inter-domain dynamics of active and inactive MMP1 using all-atom simulations (see Methods). As shown in **Figure 3A**, all-atom simulations reproduce that active MMP1 has more low FRET conformations when the collagen is restrained. The autocorrelation functions (**Figure 3B**) for simulated inter-domain distances also agree with experimental observations of higher correlation for active MMP1. Interestingly, the simulated conformational histograms (**Figure 3C**) are flipped when the collagen backbone was not restrained. In addition, the difference in autocorrelations for active and inactive MMP1 on unrestrained collagen (**Figure 3D**) is significantly lower than those on restrained collagen (**Figure 3B**). These results suggest that collagen monomers in fibrils are

bioRxiv preprint doi: https://doi.org/10.1101/804559; this version posted October 14, 2019. The copyright holder for this preprint (which was not certified by peer review) is the author/funder. All rights reserved. No reuse allowed without permission.

relatively fixed in place. Furthermore, simulations also suggest that MMP1 dynamics vary depending on the substrate properties, i.e., enzyme-substrate interactions are mutually affected by each other. Thus, experiments and simulations mutually validated each other.

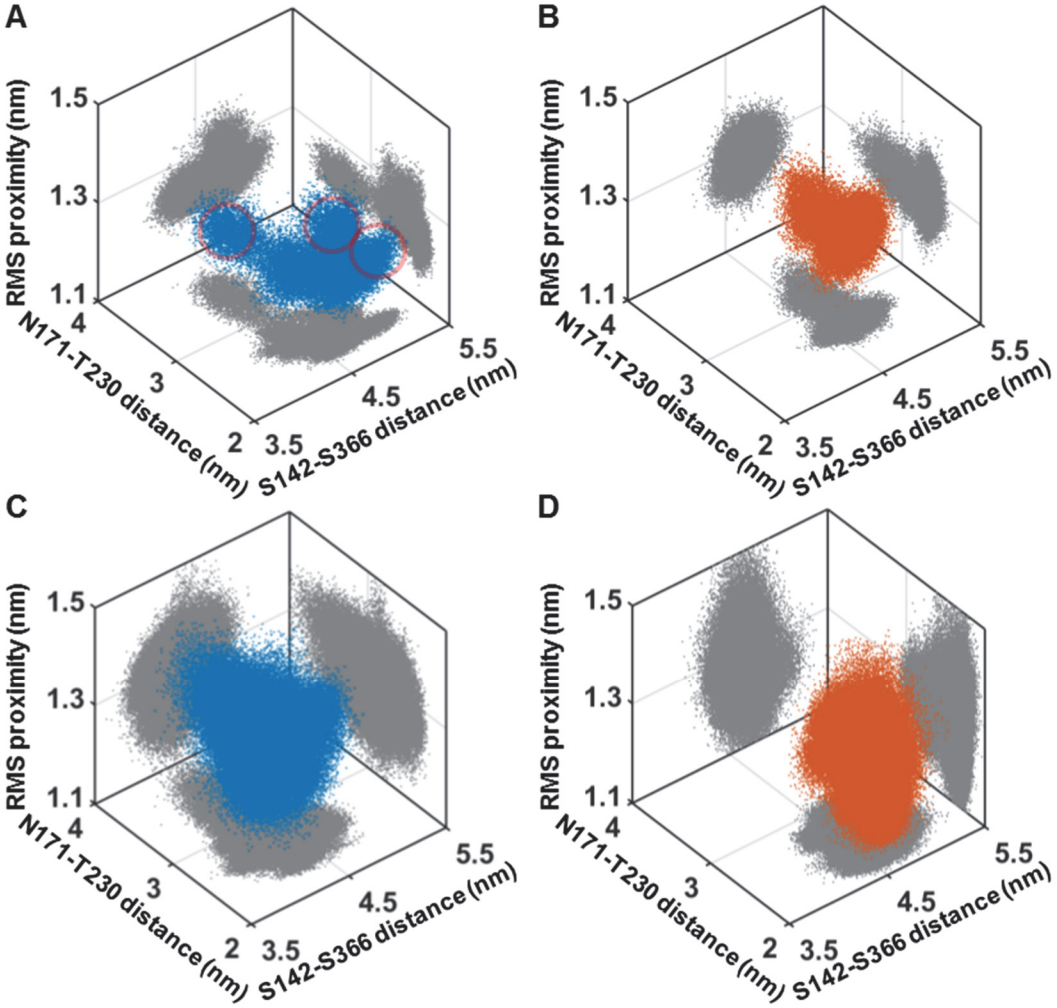

Figure 4. Insights from validated all-atom MD simulations with collagen backbone restrained (A and B) and unrestrained (C and D). Three dimensional scatter plots of S142-S366 distance (represents inter-domain dynamics), N171-T230 distance (represents the opening of the MMP1 catalytic pocket), and root mean square (rms) distance between the MMP1 catalytic site and the cleavage sites on three collagen chains for active (blue) and inactive (orange) MMP1. Two-dimensional projections of the scatter plots are in gray color. The plausible catalytically relevant conformations are indicated by the clusters encircled in red in (**A**).

Informed by single-molecule measurements of MMP1 inter-domain dynamics, we used MD simulations to identify catalytically relevant conformations more precisely. We assumed that the catalytic pocket should open up more before catalysis so that the catalytic residues can approach the cleavage sites on the three collagen chains. We measured the catalytic pocket opening by the distance between N171 and T230 and measured the proximity by the root mean square of the distances between the MMP1 residue (E/Q219) and the collagen cleavage sites (G~L). Three dimensional scatter plots (**Figure 4**) show the structures in the partial MMP1 conformational

bioRxiv preprint doi: https://doi.org/10.1101/804559; this version posted October 14, 2019. The copyright holder for this preprint (which was not certified by peer review) is the author/funder. All rights reserved. No reuse allowed without permission.

landscape. **Figure 4A** suggests that the encircled clusters are likely the functionally relevant conformations of MMP1 because these conformations are significantly absent in inactive MMP1 (**Figure 4B**). When the collagen backbone is not restrained, the finer structures of the conformational space disappear (**Figures 4C** and **4D**). Interestingly, the number of conformational peaks depends on the projection plane (reaction coordinates). Overall, the preponderance of evidence suggests that a larger inter-domain distance is critical for MMP1 activity.

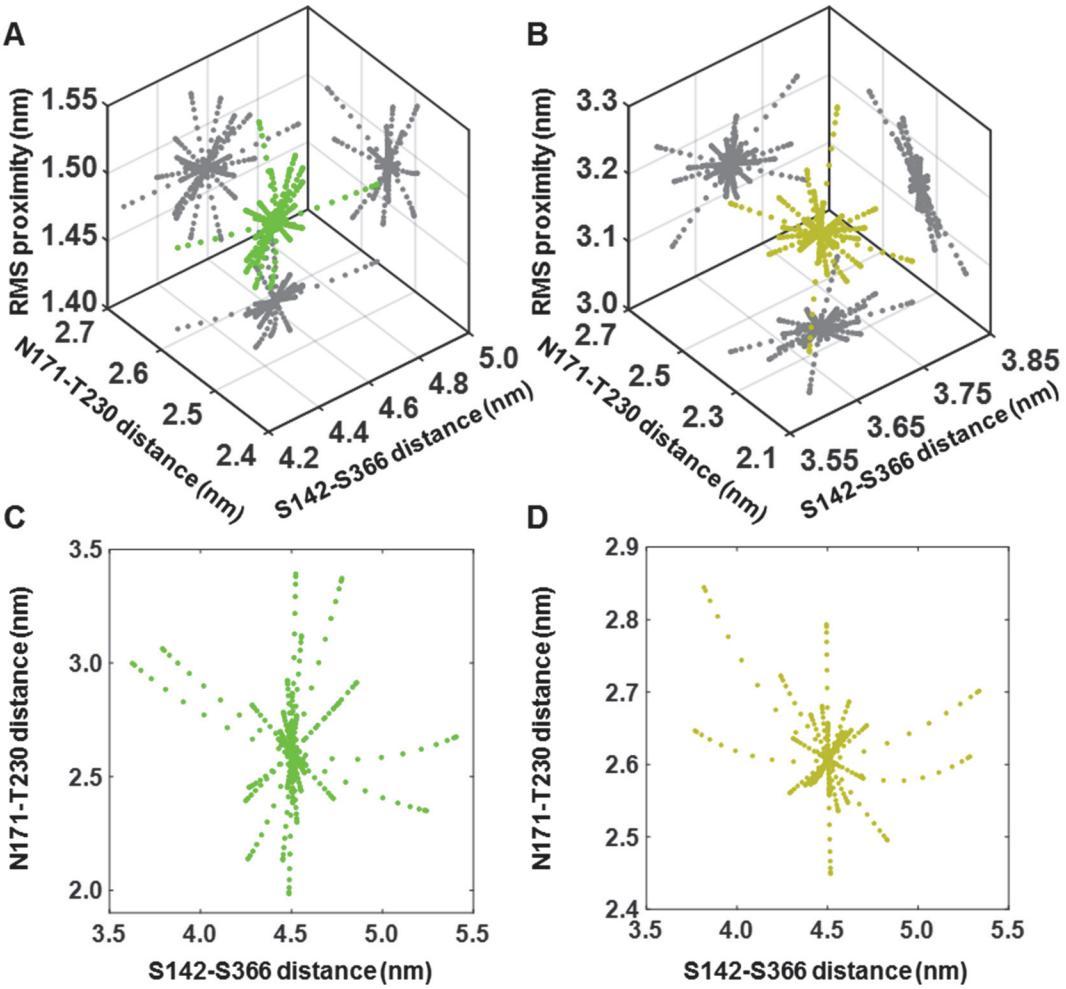

Figure 5. Normal mode analysis of MMP1 using the Anisotropic Network Model. Three dimensional scatter plots of S142-S366 distance (represents inter-domain dynamics), N171-T230 distance (represents opening of the MMP1 catalytic pocket), and root mean square (rms) distance between the MMP1 catalytic site and the cleavage sites on three collagen chains for collagen-bound active (green) (**A**) and pro (greenish-yellow) MMP1 (**B**). Two-dimensional projections in **A** and **B** of the scatter plots are in gray color. Two dimensional scatter plots of S142-S366 distance and N171-T230 distance for free active (green) (**C**) and pro (greenish-yellow) MMP1 (**D**).

On the one hand, simulations were performed starting from the crystal structure of collagen-bound MMP1, which is generally the most favorable conformations thermodynamically and kinetically. On the other hand, smFRET measurements are performed on collagen-bound MMP1, which also provides favored states. As such, functionally relevant MMP1 inter-domain conformations appear at the two extreme timescales quickly. Both the experiments (**Figure 2**) on collagen fibrils at 100

bioRxiv preprint doi: https://doi.org/10.1101/804559; this version posted October 14, 2019. The copyright holder for this preprint (which was not certified by peer review) is the author/funder. All rights reserved. No reuse allowed without permission.

ms timescale and the simulations (**Figure 4**) with collagen monomer at 5 ps timescale showed that active MMP1 adopts more conformations with larger inter-domain distances.

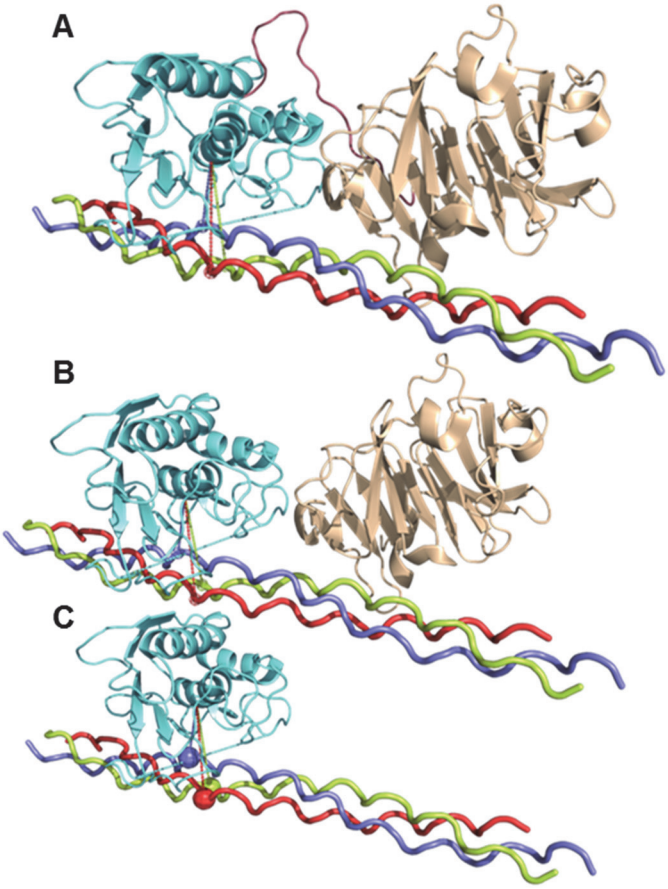

Figure 6. Inter-domain communications via collagen even without the linker. ANM simulations of the catalytic pocket opening as measured by the distance between N171 and T230 (cyan line) is (**A**) 2.56±0.52 nm, (**B**) 2.56±0.26, and (**C**) 2.55±0.19. The error bars represent the standard deviations of top three normal modes as measured by the catalytic pocket opening. The catalytic domain (cyan), the linker (brown), and the hemopexin (wheat) domains are defined between the residues V101 and Y260, G261 and C278, and D279 and C466 respectively.

Further, MMP1 is not static at the most favored conformation as envisioned in "lock-and-key", "induced fit", and "conformational selection" theories of enzyme specificity and function. Rather, MMP1 undergoes conformational dynamics that have two dynamic parts: one that has conformations with functionally relevant larger inter-domain distances and the other without functionally relevant conformations. It is often considered that a protein has a set of allowed conformations and a ligand selects the compatible protein conformation from this set. For MMP1, however, ligand binding can change the set of allowed conformations. Therefore, an alternative model of "adaptive conformational dynamics" can be proposed where the substrate recognition and function of a protein is dynamically influenced by mutations and ligands. In addition, the mutation E219Q at the catalytic site of MMP1 also changes the set of allowed conformations that appear at the two extreme timescales of all-atom simulations (**Figures 3** and **4**) and experiments (**Figure 2**).

bioRxiv preprint doi: https://doi.org/10.1101/804559; this version posted October 14, 2019. The copyright holder for this preprint (which was not certified by peer review) is the author/funder. All rights reserved. No reuse allowed without permission.

Inter-domain communications are facilitated by both the linker and the collagen substrate. To gain more insights faster, we computed preferred conformations or "normal modes" of collagen-bound MMP1 using the Anisotropic Network Model (ANM)[32]. The ANM is a prediction method that models each amino acid as a bead and creates a virtual bond network that connects these beads based on a user-defined cut-off distance[32,33]. By modeling these virtual bonds using the harmonic oscillator model, we obtained an integrated view of the restrictions in conformational space experienced by each bead and in turn, predicted what motions are accessible to MMP1. ANM cannot distinguish between active and inactive MMP1. Therefore, we calculated normal modes for proMMP1 as a proxy for inactive MMP1 because pro MMP1 cannot degrade collagen-like inactive MMP1. As such, we expected that the catalytic pocket opening and proximity to the collagen chains for proMMP1 would be restricted. We calculated normal modes for collagen-bound (**Figures 5A** and **5B**) and free (**Figures 5C** and **5D**) MMP1 for active and pro MMP1. As shown in **Figure 5**, free and collagen-bound MMP1 have some similarities in allowed normal modes but some modes of free MMP1 disappear and some new modes appear for collagen-bound MMP1. For active MMP1, the catalytically relevant intra- and inter-domain distances from ANM simulations (**Figure 5A**) agreed well with those from all-atom simulations (**Figure 4A**). When MMP1 was not bound, the ANM calculations showed different normal modes for both active (**Figure 5C**) and pro (**Figure 5D**) compared to the collagen-bound MMP1. These results further confirmed that the collagen substrate can significantly change MMP1 dynamics and validated the ANM simulations. We then investigated if the communications between the catalytic and hemopexin domains can be communicated by both the linker and collagen. **Figure 6** shows that the catalytic domain opening has the largest standard deviation when both the linker and collagen are present (**Figure 6A**) and has the smallest standard deviation when only the catalytic domain is present (**Figure 6C**), which suggest the essential role of the hemopexin domain in MMP1 activity. To confirm further, we computed conformations without the linker and observed that the hemopexin domain can still influence the catalytic domain plausibly via collagen and increase the catalytic pocket opening (**Figure 6B**). In other words, the two MMP1 domains can communicate via the linker as well as collagen. Interestingly, it has been reported previously that a mixture of the two MMP1 domains purified separately can degrade triple-helical collagen[4] but the reason was not clear. A larger catalytic opening due to allosteric communications between the two MMP1 domains via collagen provides an explanation why even a mixture of the two MMP1 domains can degrade triple-helical collagen. While autocorrelation functions are simple measures of randomness, entropy is another measure of randomness that connects to kinetics and thermodynamics. Any correlated motion or stabilization of conformations indicates a decrease in randomness (entropy). Enabling access to the cleavage sites on triple-helical collagen via inter-domain dynamics of MMP1 is an entropy-driven process.

In summary, we have measured the inter-domain dynamics of MMP1 at the single-molecule level with and without ligands. Both coarse-grained ANM simulations and all-atom MD simulations were validated by single-molecule measurements and new insights into the MMP1 dynamics were obtained from validated simulations. Larger inter-domain motion of MMP1 is accompanied by a larger catalytic pocket opening of the catalytic domain and a smaller rms distance between the MMP1 catalytic site and the cleavage sites on collagen. The allosteric approach to modulate function will be applicable to other multidomain proteins including surface receptors, enzymes, and intracellular signaling proteins.

bioRxiv preprint doi: https://doi.org/10.1101/804559; this version posted October 14, 2019. The copyright holder for this preprint (which was not certified by peer review) is the author/funder. All rights reserved. No reuse allowed without permission.

METHODS SUMMARY

Purification, labeling, and ensemble activity measurements of MMPs. Full-length recombinant MMPs were expressed in *E. coli* and purified in activated form using a protease based purification method[13]. Purified MMP1 was labeled with AlexaFluor555 (donor dye) and AlexaFluor647 (acceptor dye) using maleimide chemistry. 1 mL of MMP1 at 1 mg/mL concentration was incubated with 20 µL of 1 mg/mL AlexaFluor555 and AlexaFluor647 for 60 minutes in a 5 mL glass vial with continuous nitrogen flow to avoid oxidation of the dyes. After incubation, the sample was filtered three times using a 30 kDa cut-off Amicon filter to remove free dyes from the solution. The labeled MMP1 was analyzed using 12% SDS PAGE and the activity of labeled MMP1 was compared with the activity of unlabeled protein on the synthetic substrate, MCA-Lys-Pro-Leu-Gly-Leu-DPA-Ala-Arg-NH2, (R&D Systems, Cat# ES010) as described before[13].

Single-molecule measurements. A thin layer of reconstituted type-1 collagen fibrils was created on a quartz slide by neutralizing the solution of type-1 collagen monomers and incubating at 37°C. Alexa555 dyes attached to MMP1 was excited at 532 nm inside a flow cell made from double-sided tape sandwiched between the quartz slide and a glass coverslip using the evanescent wave created at the interface of the quartz slide and sample in a Total Internal Reflection Fluorescence (TIRF) Microscope as described before[9,10]. Alexa647 and Alexa555 emissions were imaged by two quadrants of an EMCCD camera (Andor iXon). Two emission channels were superimposed using a pairwise stitching plugin of ImageJ and the emission intensities from the two dyes were extracted and analyzed using Matlab.

Normal mode analysis using Anisotropic Network Model. Anisotropic Network Model (ANM) calculations were performed on the first biological assembly (chains A, C-E) of the crystal structure of MMP-1 in complex with a triple-helical collagen peptide (PDB: 4UAO, [PMID: 22761315]) using ANM web server 2.1 [PMID: 25568280] with default parameters. Three-dimensional fluctuation model coordinate files were obtained for the 20 slowest modes requesting 20 frames per model. For each frame on each model, selected distances were calculated using Pymol [The PyMOL Molecular Graphics System, Version 1.8, Schrödinger, LLC]. Distances between S142 and S366 were used to analyze the fluctuations between the catalytic and hemopexin domains; between N171 and T230 to analyze the fluctuations corresponding to the opening and closing of the catalytic site; and between A219 and the cleaving site in each collagen chain (defined as the middle point of the segment between G975 and C976 alpha carbons) to analyse the cleaving potential of each of the 20 slowest modes.

All-atom molecular dynamics simulations. All-atom Molecular Dynamics (MD) simulations were performed using GROMACS version 2018.2[34]. A leapfrog integration time step of 2 fs was applied and all bonded interactions were constrained using the LINCS constraint algorithm[35]. The short-range neighbor interaction list cut-off was updated every 10 fs and fixed to 0.8 nm. Short-range interactions were modeled using a 12-6 Lennard-Jones potential truncated at 0.8 nm and electrostatic interactions were truncated at 0.8 nm. Long-range electrostatic interactions were calculated using the Particle Mesh Ewald scheme[36]. Using the Nose-Hoover thermostat the temperature was maintained at 310 K[37] and by applying an isotropic coupling Parrinello-Rahman scheme[38] the pressure was maintained at one atmosphere. The simulation cell was defined using periodic boundary conditions in three dimensions. The coordinates, velocities, and energies were saved every 5 ps. We used the crystal structure (PDB ID 4AUO) of inactive MMP1 (E219A) bound to model triple-helical collagen monomer. We modified residues to match the amino acid sequences of active and inactive MMP1 used in smFRET experiments. Two cysteine to serine

bioRxiv preprint doi: https://doi.org/10.1101/804559; this version posted October 14, 2019. The copyright holder for this preprint (which was not certified by peer review) is the author/funder. All rights reserved. No reuse allowed without permission.

substitutions (C142S and C366S) used for labeling MMP1 were incorporated in the structure as well for simulations. Additionally, an alanine to glutamine substitution A219Q was incorporated to match the sequence of inactive MMP1. The initial collagen-bound MMP1 complex crystal structure (4AUO), along with the parameterization and implementation steps for the bond distances and angles, respective force constants and partial charges of the zinc-binding sites were repeated as discussed in earlier work[39]. Amino acid substitutions were performed using Schrödinger Maestro (Schrödinger Release 2015-4). Each protein complex was centered in a cubic unit cell sufficiently large enough to avoid periodic boundary artifacts. Both unit cells were solvated used TIP4P water molecules and counterions were added to neutralize the system. Both solvated protein-complex systems were subjected to a steepest descent energy minimization with a maximum force of 1000 kJ/mol stopping criteria to correct for steric clashes between atoms. Position restraints of 1000 kJ/mol were applied to all protein heavy atoms and both minimized structures underwent a 10 ps molecular dynamics simulation using the NVT (fixed particles, volume, and temperature) ensemble. The position restraints were maintained and the simulation was extended by 200 ps with constant pressure using the Parrinello-Rahman pressure coupling scheme. Each simulation was extended by a series of 200 ps intervals, systematically reducing the position restraints by an order of magnitude to a final 10 kJ/mol. All position restraints were removed with the exception to those on the collagen alpha-carbon atoms which were increased to 150 kJ/mol. This was to prevent the fraying of the short collagen whilst the structure relaxed. Both systems underwent a 300 ns NPT (fixed particles, pressure and temperature) production simulation. The position restraints were removed from the collagen alpha-carbon and both systems underwent a further 700 ns of NPT simulation time for a total simulation time of 1 μs.

ACKNOWLEDGMENTS

The authors acknowledge John Czerski and Danielle Forristall for participating in the initial stage of single-molecule FRET measurements and analyses.

AUTHOR CONTRIBUTIONS

S.K.S. conceived and designed the overall project. L.K. and S.K.S. designed experiments. L.K. performed experiments. A.N. performed all-atom simulations. C.H. wrote codes for analyzing smFRET. J.P. performed ANM simulations and molecular docking. L.K., A.N., J.P., D.R., J.K.S., and S.K.S. analyzed data. S.K.S. wrote the initial manuscript. All authors read and edited the manuscript.

COMPETING FINANCIAL INTERESTS

The authors declare no competing financial interests.

bioRxiv preprint doi: https://doi.org/10.1101/804559; this version posted October 14, 2019. The copyright holder for this preprint (which was not certified by peer review) is the author/funder. All rights reserved. No reuse allowed without permission.

1 Karplus, M. Role of conformation transitions in adenylate kinase. *Proceedings of the National Academy of Sciences* **107**, E71-E71 (2010).

2 Pisliakov, A. V., Cao, J., Kamerlin, S. C. & Warshel, A. Enzyme millisecond conformational dynamics do not catalyze the chemical step. *Proceedings of the National Academy of Sciences* **106**, 17359-17364 (2009).

3 Henzler-Wildman, K. A. *et al.* A hierarchy of timescales in protein dynamics is linked to enzyme catalysis. *Nature* **450**, 913 (2007).

4 Chung, L. D. *et al.* Collagenase unwinds triple-helical collagen prior to peptide bond hydrolysis. *Embo Journal* **23**, 3020-3030 (2004).

5 Manka, S. W. *et al.* Structural insights into triple-helical collagen cleavage by matrix metalloproteinase 1. *Proc Natl Acad Sci U S A* **109**, 12461-12466, doi:10.1073/pnas.1204991109 (2012).

6 Nerenberg, P. S., Salsas-Escat, R. & Stultz, C. M. Do collagenases unwind triple-helical collagen before peptide bond hydrolysis? Reinterpreting experimental observations with mathematical models. *Proteins: Structure, Function, and Bioinformatics* **70**, 1154-1161 (2008).

7 Leikina, E., Mertts, M. V., Kuznetsova, N. & Leikin, S. Type I collagen is thermally unstable at body temperature. *Proceedings of the National Academy of Sciences of the United States of America* **99**, 1314-1318 (2002).

8 Karabencheva-Christova, T. G., Christov, C. Z. & Fields, G. B. Conformational Dynamics of Matrix Metalloproteinase-1· Triple-Helical Peptide Complexes. *The Journal of Physical Chemistry B* (2017).

9 Dittmore, A. *et al.* Internal strain drives spontaneous periodic buckling in collagen and regulates remodeling. *Proceedings of the National Academy of Sciences*, 201523228 (2016).

10 Sarkar, S. K., Marmer, B., Goldberg, G. & Neuman, K. C. Single-molecule tracking of collagenase on native type I collagen fibrils reveals degradation mechanism. *Current biology : CB* **22**, 1047-1056, doi:10.1016/j.cub.2012.04.012 (2012).

11 Perumal, S., Antipova, O. & Orgel, J. P. R. O. Collagen fibril architecture, domain organization, and triple-helical conformation govern its proteolysis. *Proceedings of the National Academy of Sciences of the United States of America* **105**, 2824-2829 (2008).

12 Saffarian, S., Collier, I. E., Marmer, B. L., Elson, E. L. & Goldberg, G. Interstitial collagenase is a Brownian ratchet driven by proteolysis of collagen. *Science* **306**, 108-111 (2004).

13 Kumar, L., Colomb, W., Czerski, J., Cox, C. R. & Sarkar, S. K. Efficient protease based purification of recombinant matrix metalloprotease-1 in E. coli. *Protein expression and purification* **148**, 59-67 (2018).

14 Neumann, U., Kubota, H., Frei, K., Ganu, V. & Leppert, D. Characterization of Mca-Lys-Pro-Leu-Gly-Leu-Dpa-Ala-Arg-NH2, a fluorogenic substrate with increased specificity constants for collagenases and tumor necrosis factor converting enzyme. *Analytical biochemistry* **328**, 166-173 (2004).

15 Kamerlin, S. C. & Warshel, A. Reply to Karplus: Conformational dynamics have no role in the chemical step. *Proceedings of the National Academy of Sciences* **107**, E72-E72 (2010).

bioRxiv preprint doi: https://doi.org/10.1101/804559; this version posted October 14, 2019. The copyright holder for this preprint (which was not certified by peer review) is the author/funder. All rights reserved. No reuse allowed without permission.

16 Patterson, M. L., Atkinson, S. J., Knäuper, V. & Murphy, G. Specific collagenolysis by gelatinase A, MMP-2, is determined by the hemopexin domain and not the fibronectin-like domain. *FEBS letters* **503**, 158-162 (2001).

17 Saito, S. *et al.* Role of matrix metalloproteinases 1, 2, and 9 and tissue inhibitor of matrix metalloproteinase-1 in chronic venous insufficiency. *Journal of Vascular Surgery* **34**, 930-937 (2001).

18 Asahi, M. *et al.* Role for matrix metalloproteinase 9 after focal cerebral ischemia, effects of gene knockout and enzyme inhibition with BB-94. *Journal of Cerebral Blood Flow and Metabolism* **20**, 1681-1689 (2000).

19 Fujimura, M. *et al.* Early appearance of activated matrix metalloproteinase-9 and blood-brain barrier disruption in mice after focal cerebral ischemia and reperfusion. *Brain Research* **842**, 92-100 (1999).

20 Hanemaaijer, R., Visser, H., Konttinen, Y. T., Koolwijk, P. & Verheijen, J. H. A novel and simple immunocapture assay for determination of gelatinase-B (MMP-9) activities in biological fluids: Saliva from patients with Sjogren's syndrome contain increased latent and active gelatinase-B levels. *Matrix Biology* **17**, 657-665 (1998).

21 Koshiba, T. *et al.* Detection of matrix metalloproteinase activity in human pancreatic cancer. *Surgery Today-the Japanese Journal of Surgery* **27**, 302-304 (1997).

22 Sakalihasan, N., Delvenne, P., Nusgens, B. V., Limet, R. & Lapiere, C. M. Activated forms of MMP(2) and MMP(9) in abdominal aortic aneurysms. *Journal of Vascular Surgery* **24**, 127-133 (1996).

23 Goldberg, G. I., Strongin, A., Collier, I., Genrich, L. & Marmer, B. Interaction of 92-kDa type IV collagenase with the tissue inhibitor of metalloproteinases prevents dimerization, complex formation with interstitial collagenase, and activation of the proenzyme with stromelysin. *Journal of Biological Chemistry* **267**, 4583-4591 (1992).

24 Powell, B., Malaspina, D. C., Szleifer, I. & Dhaher, Y. Effect of collagenase–gelatinase ratio on the mechanical properties of a collagen fibril: a combined Monte Carlo–molecular dynamics study. *Biomechanics and modeling in mechanobiology*, 1-11 (2019).

25 Golub, L. *et al.* Tetracyclines inhibit tissue collagenase activity. *Journal of periodontal research* **19**, 651-655 (1984).

26 Jarymowycz, V. A. & Stone, M. J. Fast time scale dynamics of protein backbones: NMR relaxation methods, applications, and functional consequences. *Chemical reviews* **106**, 1624-1671 (2006).

27 Singh, W., Fields, G. B., Christov, C. Z. & Karabencheva-Christova, T. G. Importance of the Linker Region in Matrix Metalloproteinase-1 Domain Interactions. *RSC advances* **6**, 23223-23232, doi:10.1039/C6RA03033E (2016).

28 Ratnikov, B. I. *et al.* Basis for substrate recognition and distinction by matrix metalloproteinases. *Proceedings of the National Academy of Sciences* **111**, E4148-E4155 (2014).

29 Piccard, H., Van den Steen, P. E. & Opdenakker, G. Hemopexin domains as multifunctional liganding modules in matrix metalloproteinases and other proteins. *Journal of leukocyte biology* **81**, 870-892 (2007).

30 Overall, C. M. Molecular determinants of metalloproteinase substrate specificity. *Molecular biotechnology* **22**, 51-86 (2002).

31 Clark, I. M. & Cawston, T. E. Fragments of human fibroblast collagenase. Purification and characterization. *Biochemical Journal* **263**, 201-206 (1989).

bioRxiv preprint doi: https://doi.org/10.1101/804559; this version posted October 14, 2019. The copyright holder for this preprint (which was not certified by peer review) is the author/funder. All rights reserved. No reuse allowed without permission.

32 Eyal, E., Yang, L.-W. & Bahar, I. Anisotropic network model: systematic evaluation and a new web interface. *Bioinformatics* **22**, 2619-2627 (2006).

33 Isin, B., Tirupula, K. C., Oltvai, Z. N., Klein-Seetharaman, J. & Bahar, I. in *Membrane Protein Structure and Dynamics* 285-317 (Springer, 2012).

34 Abraham, M. J. *et al.* GROMACS: High performance molecular simulations through multi-level parallelism from laptops to supercomputers. *SoftwareX* **1**, 19-25 (2015).

35 Hess, B., Bekker, H., Berendsen, H. J. & Fraaije, J. G. LINCS: a linear constraint solver for molecular simulations. *Journal of computational chemistry* **18**, 1463-1472 (1997).

36 Darden, T., York, D. & Pedersen, L. Particle mesh Ewald: An N· log (N) method for Ewald sums in large systems. *The Journal of chemical physics* **98**, 10089-10092 (1993).

37 Hoover, W. G. Canonical dynamics: Equilibrium phase-space distributions. *Physical review A* **31**, 1695 (1985).

38 Parrinello, M. & Rahman, A. Polymorphic transitions in single crystals: A new molecular dynamics method. *Journal of Applied physics* **52**, 7182-7190 (1981).

39 Nash, A., Birch, H. L. & de Leeuw, N. H. Mapping intermolecular interactions and active site conformations: from human MMP-1 crystal structure to molecular dynamics free energy calculations. *Journal of Biomolecular Structure and Dynamics* **35**, 564-573 (2017).